Eur. Phys. J. B **35**, 125–132 (2003)
DOI: 10.1140/epjb/e2003-00263-7

THE EUROPEAN PHYSICAL JOURNAL B

Adsorption of oxygen on Si(100) steps: a study at semiempirical level

A.M. Mazzone[a]

C.N.R.-Istituto IMM, Sezione di Bologna, Via Gobetti 101, 40129 Bologna, Italy

Received 30 April 2003 / Received in final form 24 July 2003
Published online 22 September 2003 –

Abstract. In this study oxygen adsorption on steps of the Si(100) surface is investigated with quantum mechanical detail. A cluster model represents the step structure and the oxygen impurity is deposited in this cluster above the dimer rows. A map of the total energy sensed by the adsorbate is constructed by displacing the oxygen atom on the terraces and down the step and allowing the system to relax to the total-energy-optimized configuration by a steepest-descent method. A self-consistent semiempirical molecular orbital method is applied to the evaluation of the total energy. Though the adsorption geometries are reminiscent of the ones observed for the flat surface, the effects of the step geometry are noticeable. They influence both the preferred adsorption sites and the properties of the electronic configuration of the adsorbed system.

PACS. 68.43.Fg Adsorbate structure (binding sites, geometry) – 68.90.+g Other topics in structure, and nonelectronic properties of surfaces and interfaces; thin films and low-dimensional structures (restricted to new topics in section 68) – 07.05.Tp Computer modeling and simulation

1 Introduction

The oxidation of silicon has attracted a great deal of attention over the years due to the technological importance of silicon oxide thin films for the fabrication of microelectronic devices. Though great progress has been made in this field it is generally acknowledged that much is still to be understood regarding the atomistic detail of the oxidation processes.

While H_2O has been widely used as the oxidizing agent for silicon, O_2 has become the species of choice for gate oxides as its oxidation rate is slower than that of H_2O resulting in a better control of the oxide thickness and thinner films. In the intensive experimental investigation carried out in this field microscopy techniques, like Scanning Reflection Electron Microscopy and Electron Energy Loss Spectroscopy, have been generally applied to the first stages of the oxidation process. These experiments have demonstrated that there are two distinct adsorption mechanisms at different incident kinetic energy regimes. At low incident kinetic energy the adsorption of oxygen on silicon proceeds through precursor-mediated species followed by the dissociation of O_2 on the surface. In the high kinetic energy regime a direct chemisorption mechanism in which the O_2 molecule dissociates immediately upon adsorption dominates. At high temperature the desorption channel of volatile SiO also opens (see [1,2] and Refs. therein). In addition to this oxidation-induced etching, oxide-cluster nucleation also occurs and produces visible clusters which can be directly counted. This allows an accurate determination of their kinetics of growth.

The effect of the growth conditions on the nucleation of the oxygen clusters has been studied in great detail for both flat and vicinal Si(100) using Scanning Tunneling Microscopy [3–5]. For vicinal surfaces these studies [5] show that the concentration of clusters increases linearly with the increase of the miscut angle θ up to $\theta \sim 4°$. Above this angle the nucleation remains roughly constant or possibly starts to decrease. In [5] the effect is explained in terms of the competition between the oxygen diffusion length and the width of the steps. However it is known that the structure of Si(100) is a complex function of the miscut angle and of the temperature. At $\theta \leq 1°$ the surface retains a nearly flat shape being formed by steps of a monolayer height. The increase of θ leads to the increase of the step height with a progression from monolayer to mounded structures at $\theta \geq 6°$. The dependence on θ of the cluster nucleation implicitly indicates a dependence of the oxygen reactivity on the step structure, which is also suggested in [5].

To clarify the existence of these effects at atomistic level several issues, like preferential adsorption sites on steps, their dependence on the step structure and the electronic quality of the oxygen-step bond, require to be

[a] e-mail: mazzone@bo.imm.cnr.it

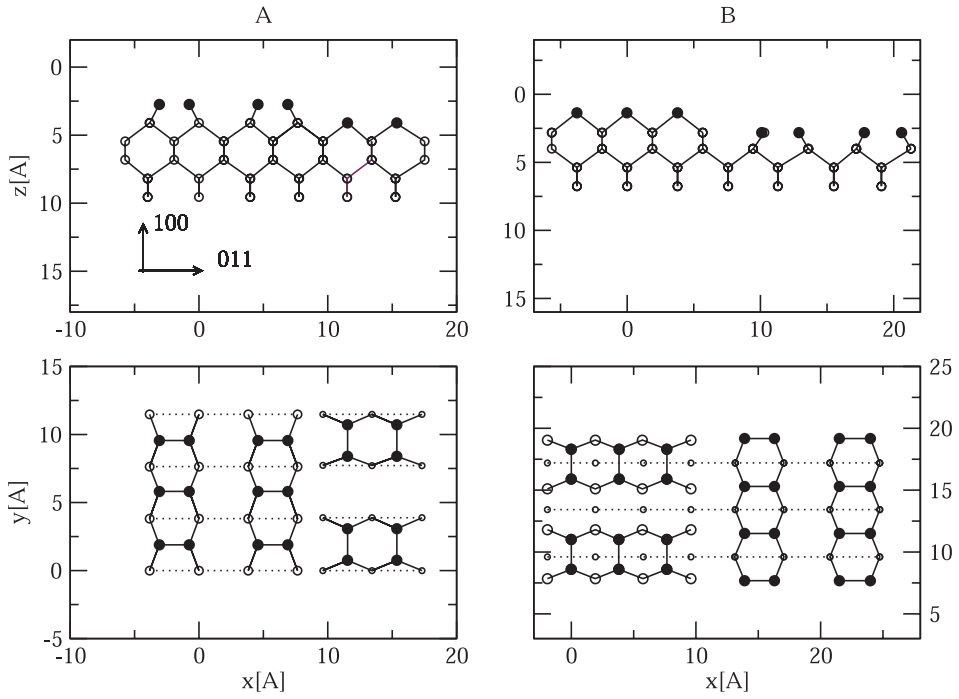

Fig. 1. SA step B: SBN step. A side and top view is given in the top and bottom panels, respectively. Dimers are marked by black circles. In the top view open circles mark subsurface atoms and the circle size decreases with the increase of the distance from the surface. Both views show bonding between dimers and subsurface atoms.

studied. The purpose of this paper is to investigate these aspects of oxygen adsorption.

It is known that adsorption represents a subtle topic in computational physics as one has to trace the minute effects arising from the deposited atom against the massive contributions of the substrate. Bare clusters formed by extracting a lattice fragment from the surface have been widely adopted. The use of such a model (thereafter indicated as Cluster Model or CM) is justified because the adsorption of an atom or a molecule can be considered as a local interaction. The region far from the site of adsorption is not disturbed and is therefore simply neglected. CM has been widely applied to the reconstruction of Si(100) and Si(111) and boron segregation on these surfaces (see [8] and Refs. therein). On the contrary, a supercell geometry has been used to study oxygen adsorption on Si(100) (see [1,9–11] and Refs. therein). However in [2] the initial decomposition of O_2 is based on CM and this justifies the adoption of this model in the present work.

The clusters used in the following calculations contain a number of dimers and subsurface atoms sufficient to realistically describe distant interactions on the surface and below it. A map of the energy sensed by the deposited oxygen is obtained by displacing the atom on the terraces and down the step. This allows to identify preferred adsorption sites and to study their dependence on the step structure.

The plan of the work is as follows. Section 2 describes the structures used in the simulation and the semiempirical Hamiltonian. In Section 3 calculations on small oxygen-silicon clusters are reported. These calculations offer insight onto the properties of the oxygen-silicon bond and represent a benchmark of the quality of the semiempirical Hamiltonian. This section reports also data on the clean steps. The properties of oxygen-adsorbed steps are presented in Section 4.

2 Computational details

The simulation cell reproduces the structures observed on Si(100) cut with $\theta \leq 1^\circ$ with respect to (100) at low temperature. Under these conditions the steps have a monoatomic height and the exposed surface on the terraces reconstructs by the formation of dimerized rows, which is also the reconstruction on the flat surface. However the dimerization axis in the steps rotates 90° from the upper to the lower terrace.

According to the Chadi's nomenclature [12] there are only two types of monolayer steps: one where the step edge is parallel to the dimer row in an upper edge and one where it is normal, labeled SA and SB, respectively. Furthermore there is a possibility of forming pentagons at the step edge to saturate the dangling bonds (this structure is indicated as rebonded step). Whether the rebonded structure has lower energy than the nonrebonded one is, however, subtle due to the bond-length strains in the Si pentagons in the rebonded structure. The steps chosen for the following calculations are of the SA and SB non-rebonded type (indicated as SBN). A top and side view of the two steps is presented in Figure 1. The figure clearly shows that the lattice locations along the x direction, perpendicular to the step edge, are not equivalent and therefore the energy

of the system E_t has a functional dependence on both x and z. This represents the central difference between the step and the flat surface, where E_t depends only on z, and constitutes the essence of the step effect. Furthermore the width of the empty region at the step edge is different for SA and SBN and, as shown below, this difference has profound effects on adsorption.

Despite its simplicity, the cluster model has been used with remarkable success to predict properties such as geometries and frequencies of adsorbed molecules. However, depending on the property studied, the accuracy of the results depends strongly on the size of the cluster. The binding energies, for example, converge very slowly with increasing size. This failure arises from boundary effects, which cause an unequal charge distribution within the cluster. In the chemical literature several approaches improve upon the bare cluster by embedding it into a suitable bath [13]. The boundary conditions used in this study have been taken from [2] but their use is widespread in the silicon literature. Accordingly, the dangling bonds due to the truncated bulk silicon bonds are terminated with hydrogen atoms which are constrained to lie in a tetrahedral location with a distance ∼1.5 Å from silicon atoms. The clusters size n consists on approximately 120 silicon atoms. The step thickness reaches six layers below the upper terrace and there are three-four dimer rows, with at least three dimers, on each terrace. To investigate size-dependent effects separate calculations have been performed using clusters with a variable number of layers down to the size $n = 40$ (in all cases the hydrogen compensation is applied from the first subsurface layer to the bottom one).

To study adsorption an oxygen atom is placed in the step at an height $z \sim 1.0$ Å above the surface. As shown below in Figure 3, locations between dimers and between dimer rows in the upper and lower terrace up to a distance of about three lattice spacings from the step edge have been tested. The evaluation of the total energy E_t is carried out by relaxing the cluster structure by a steepest descent method to a total energy minimum. In this minimization only oxygen and silicon atoms are allowed to move while the hydrogen boundary is rigid.

Owing to the size of the steps and to the number of lattice locations tested for adsorption the use of an *ab initio* wavefunction is impractical and a semiempirical Hamiltonian has to be adopted. The one used in the following calculations, known by the acronym of AM1 in the chemical literature, belongs to the Modified Neglect of Diatomic Overlap method in the restricted Hartree-Fock formulation (the software is taken from the MOPAC suite of programs [14]). Literature results indicate that this Hamiltonian successfully describes several silicon-based materials, like silicon surfaces (an extensive bibliography on this subject can be found [8,15]), silloxenic materials and compound silicon-oxygen clusters [16,17]. The overlapping and coulomb integrals, needed by the Hartree-Fock formulation, are treated at MNDO level neglecting three-centers interactions and using parameters taken from experiments. Basic parameters of this formulation are the one-center one-electron energy $U_{\mu\mu}$, the one-center two-electrons repulsion and exchange integrals $g_{\lambda\mu}$ and $h_{\lambda\mu}$, respectively, the two-center one-electron core resonance integral $\beta_{\lambda\mu}$, the two-center one-electron attraction integral $V_{\lambda\mu,\mathrm{B}}$ and the two-center two-electron repulsion integral $\langle\mu\nu,\lambda\sigma\rangle$. Here λ and μ indicate the type of atomic orbital and $V_{\lambda\mu,\mathrm{B}}$ accounts for the attraction exerted on the electrons ψ_λ,ψ_μ on the atom A by the core B. The one-center terms $U_{\mu\mu}$, $g_{\lambda\mu}$ and $h_{\lambda\mu}$ are fitted to the spectroscopic constants of the given element. The resonance integrals $\beta_{\lambda\mu}$ are proportional to the overlapping integrals $S_{\lambda\mu}$ *via* a function $f(R_{\mathrm{AB}})$ of the distance between atom A and B which is also adopted for $V_{\lambda\mu,\mathrm{B}}$. This function is parametrized to fit properties of the molecular state of the given atom. A multipole expansion with Slater exponents is used for the two-center repulsion integral $\langle\mu\nu,\lambda\sigma\rangle$. In AM1 s and p states are used for silicon and oxygen and there are 18 parameters for each atoms. For all these quantities the internal values of MOPAC [14] have been adopted.

The quantities used to define the electronic structure of the system are the adsorption energy E_a, the ionization potential I_p and the Mulliken charge on the oxygen atom Q_o. E_a is evaluated as $E_a = E_t - E_t(clean) - E_o$, where E_t and $E_t(clean)$ are the total energy in the step with and without the oxygen atom, respectively. E_o is the energy of the free oxygen atom. A negative E_a indicates binding and the increase of the step binding action leads to a decrease of E_a. Q_o is the electronic charge gained or lost with respect to the valence charge of the free atom.

The cluster structures reported in Section 3 are obtained from the minimization of the total energy using AM1. The binding energy E_b used in these calculations is the cluster total energy measured with respect to the energy of an equal ensemble of free atoms.

3 Test calculations: small clusters and clean steps

In the literature on silicon oxidation hypersilicon clusters have been often used to provide structural models for the oxidation of the silicon surfaces [18–20]. Therefore the study of these structures is physically meaningful and offers a relevant introduction to the properties of oxygen-adsorbed steps.

Structural properties and binding energies of small oxygen, silicon and silicon-oxygen clusters are reported in Table 1 which also resumes literature results.

The large binding energies of clusters containing oxygen are attributable to the electronegativity of this element which makes it a very strong electron withdrawing species. However the charge adsorbed by oxygen has a weak dependence on the silicon content. For instance, the value of Q_o is -0.75 for SiO, but saturates to approximately -0.80 in Si_2O and Si_3O. A feature common to all Si_nO clusters is that, while the Si-Si bond is close to the normal value in crystalline silicon (*i.e.* 2.35 Å), the Si-O distance is intermediate between the one of

Table 1. Properties of oxygen, silicon and oxygen-silicon clusters. AM1 calculations and literature results E_b, R_b and I_p indicate the binding energy, the average bond length and the ionization potential, respectively. MPn indicates a Hartree Fock formulation with Møller-Plesset perturbation theory applied to the nth order. The source of data on oxygen, silicon and hypersilicon clusters is [25,26] and [18–20], respectively.

literature results: experiment

cluster	structure	source	E_b (eV)	I_p (eV)	R_b (Å)
O_2	-	[25]	−5.22	12.07	1.21
Si_2	-	[26]	−3.21	7.40	-
Si_3	-	[26]	−7.70	-	-
SiO	-	[18,19]	−8.24	11.4	1.51

literature results: theory

cluster	structure	Hamiltonian	E_b (eV)	I_p (eV)	R_b (Å)
Si_2		HF	−1.51	-	-
Si_3	-	HF	−3.04	-	-
Si_2		HF-MP4	−3.17	7.50	2.23
Si_3	isosceles triangle	HF-MP4	−7.70	7.90	2.43
SiO		HF-MP2	−8.12	-	1.54
Si_2O	linear, Si-O-Si	”	−10.20	6.00	1.66
	triangle, Si-O-Si		−11.32	7.50	S-Si side=2.34
					Si-O side=1.72
Si_3O	rhombus		−13.91	7.68	Si-Si side=2.30
					Si-O side=1.75

AM1 calculations

cluster	structure	E_b (eV)	I_p (eV)	R_b (Å)
O_2		−5.14	13.50	1.93
Si_2		−2.92	7.20	2.28
Si_3		−8.38	8.30	2.27
SiO		−8.53	8.60	1.57
Si_2O	linear, Si-O-Si	−11.62	5.70	1.67
	triangle, Si-O-Si	−11.32	7.20	Si-Si side=2.45
				Si-O side=1.75
Si_3 O	rhombus	−14.63	7.45	Si-Si side=2.41
				Si-O side=1.81

crystalline silicon and of the O_2 molecule. This feature indicates a noticeable intermixing and hybridization of the atomic orbitals on the two atoms. Furthermore the formation of bending Si-O-Si structures provides hint that when an oxygen atom interacts with large silicon clusters, it will coordinate outside of rather than insert into such clusters. For Si_2O, in addition to S-O-Si, a Si-Si-O isomer, also reported in [18,19], was also obtained. However its energy was about 1 eV above the one of Si-O-Si. As shown below, both Si-O-Si and Si-Si-O are adsorption geometries for oxygen deposited on steps.

The AM1 evaluation of the binding energies differs of about 8% from literature data and consistent results are also obtained for I_p and the cluster geometry. However differences in the range 30% between AM1 and experiment are observed for R_b of O_2 and for I_p of SiO. The structure most divergent from the ones in the literature is Si_2O for which AM1 predicts a linear shape while it is triangular in [18]. However the structure of Si_2O is controversial (as also reported in [18]) and the linear and bent model have been often in contrapposition. The source of this divergence is the floppy angle of the Si-O bond which

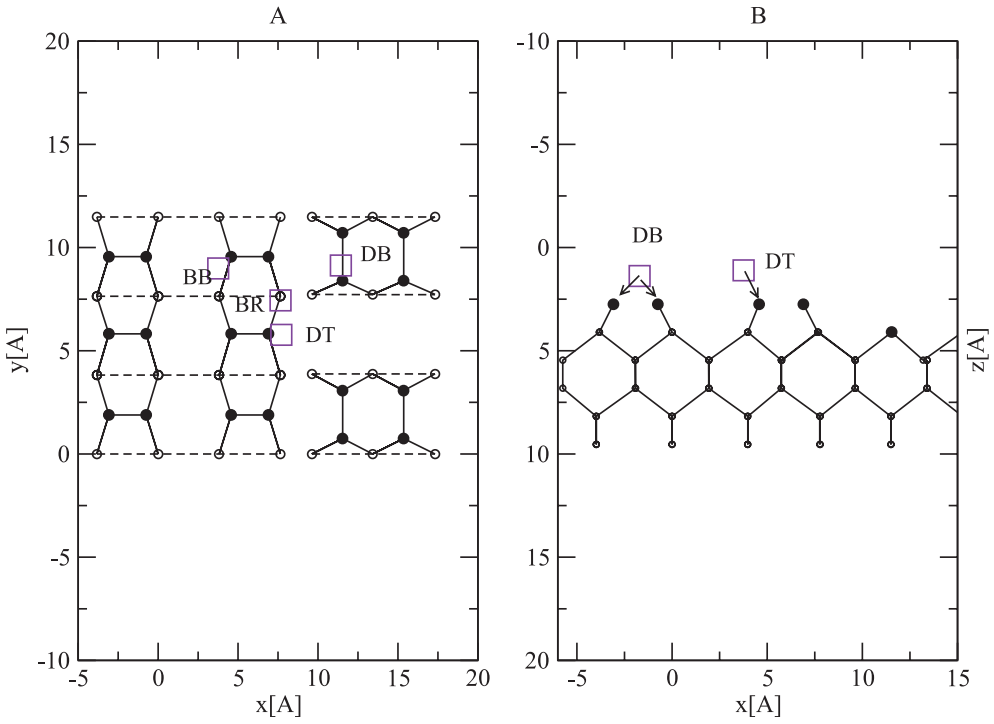

Fig. 2. The figure shows preferred adsorption sites. Top (A) and side (B) view. Oxygen are marked by the empty square whereas the convention for silicon atoms is as in Figure 1.

significantly changes according to the steering constraints imposed by the representation.

As shown by Table 1, the literature on silicon clusters indicates a critical dependence on the Hamiltonian and this suggests that the AM1 failures arise from the low order of the approach. Tests calculations using Configuration Interaction showed appreciable improvements. However the failure to converge when using a large number of microstates limits the practical applicability of these calculations and this approach was abandoned.

As a further test on the accuracy of AM1, separate calculations were performed by relaxing the clean steps to an energy minimum. Similar calculations, using Local Density Approximation or Tight Binding theory, lead to appreciably different structures depending on the quality of the Hamiltonian [21–24] and this is in itself suggestive of the difficulty of this evaluation. However there is agreement in two main points, *i.e.* (i) the distance between first and second layer atoms at the step edge is around 2.2 Å while in the other step regions the average bond lengths of crystalline silicon are approximately preserved, (ii) the strained bonds at the step edge generate a remarkable electronic coupling between the two terraces. Due to this effect, the dimerization has more complex patterns (*i.e.* $c2 \times 4$, $c2 \times 2$) than the 2×1 structure in the flat surface. Also the buckling of step edge dimers (*i.e.* the different height z of the two dimer atoms) is larger than for the flat surface (the two values are 0.7 Å and 0.5 Å, respectively)

Simulations using either the small and the large cells showed the occurrence of the two features above. However, at variance with [21,22], an irregular buckling, with values oscillating between 0.2–0.6 Å, rather than the regular domains reported in these studies, was observed. A possible explanation of this divergence is that AM1 lacks the degree of correlation required to create regular dimerization patterns. An alternative explanation can be sought in the small size of the structures used in the other studies in comparison with the ones adopted here. It is therefore possible that the use of periodic boundary conditions, in conjunction with cells of small size, has artificially enhanced the correlation among dimers. The absence of these patterns in [24] would suggest this last hypothesis to be the correct one.

4 Oxygen-adsorbed steps

The results of the calculations on adsorption are reported in Figures 2, 3 and 4. The first of these figures show preferred adsorption sites whereas the other two illustrate the effect of the steps on the adsorption energy and on the other parameters of the electronic configuration.

The calculations indicate that the adsorption site is constantly close to a dimer location and generally along a dangling orbital axis. No tendency for subsurface segregation was observed and simulations started with oxygen buried below the surface ended with the atom above it. This is in agreement with the trend toward nucleation on the surface experimentally observed [5].

As shown by the top view in Figure 2a, there are four basic adsorption geometries: (i) the oxygen resides in a site bridging between dimers (DB), (ii) on top of a dimer

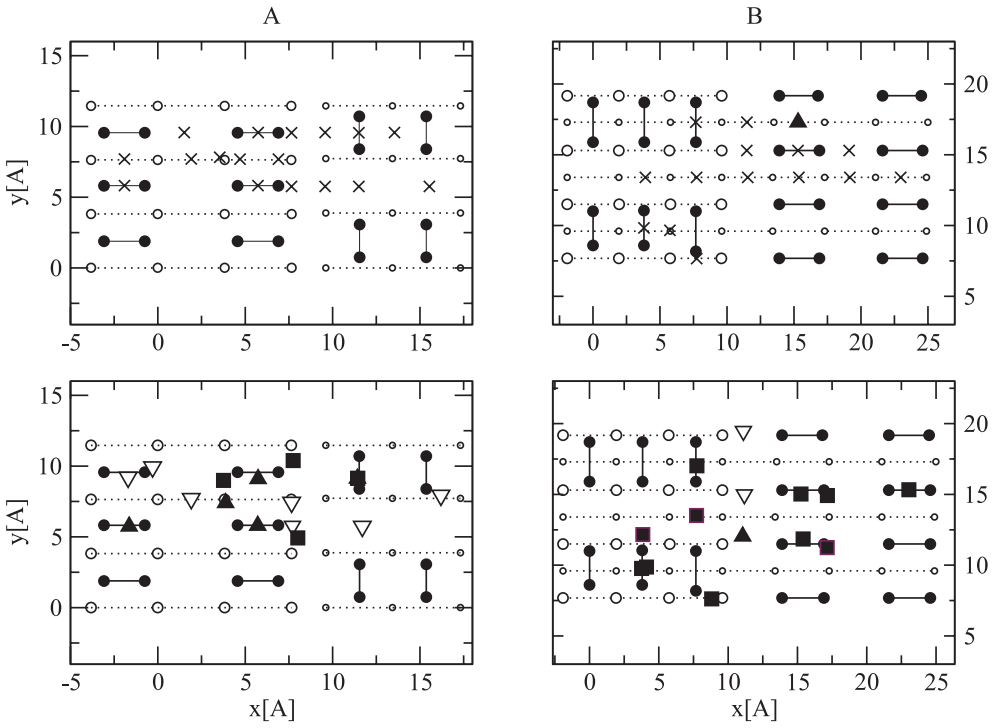

Fig. 3. The figure shows in a top view the incidence points of the adsorbed oxygen (top panels) and their final location at the end of the energy minimization (bottom panels). A: SA step. B: SBN step. The convention for dimers and subsurface atoms is as in Figure 1 but bonding is not reported. The oxygen incidence points are marked by a cross. Their final sites are marked by squares and triangles and color-coded according to their adsorption energy. The darker symbols indicate the lowest energy. The dark triangles show the adsorption minima.

atom a part from it (DT), (iii) in a back-bond between a dimer and a subsurface atom (BB) and (iiii) in a bridging site between dimer rows (BR). In the bridging sites the oxygen location is at the center of a triangle whose apexes are the silicon atoms underneath. This structure is clearly reminiscent of the Si-O-Si cluster described in the previous section whereas DT reproduces the Si-Si-O alignment (these structures are marked by arrows in Fig. 2b).

For all these configurations it has been also found that the silicon side of the structure is displaced and/or upward lifted by the electrostatic interaction with oxygen. This readjustment has a complex dependence on both the adsorption site and the step geometry and its description has been omitted for the sake of brevity.

An essential agreement exists between the geometries in Figure 2 and the ones reported for the flat surface. In fact, adsorption of atomic oxygen into the DB, DT and BB sites is reported in [10,11] using *ab initio* calculations. In addition, the studies of adsorption of the O_2 molecule indicate its decomposition into two separate atoms whose location is a DB and a BB site, respectively [1,2].

The presentation in Figure 3 is intended as a visual description of the binding action of the atomic rows rather than a precise map of the adsorption energy. Accordingly, the initial incidence points of the deposited oxygen (top panels) are compared with their final location at the end of the energy minimization (bottom panels). The final sites are marked by squares and triangles and color-coded according to their adsorption energy. The darker symbols indicate the lower values of E_a and the patterned triangles show the adsorption minima. The important aspects in these calculations are two. First, the lower panels are noticeably emptier than the upper ones. This indicates that oxygen has moved to the same adsorption site from different initial locations. Sites represented by the same point in the plots have often coordinates differing of a few tenths of Å and this difference does not appear on the scale of the figures. However the E_a values in these sites are perceptibly different. This feature is important. It demonstrates that adsorption is a complex function with different minima closely located in space.

Second, the relevant result in the context of this study is the difference between the two steps. In fact, while the SA ledge is a poor sink and the adsorption sites are concentrated on the terraces, the SBN ledge is a strong sink and many adsorption sites are allowed at its step edge. In these sites E_a has large fluctuations (shown by the different colors of the data points) arising from the different modes of lattice relaxation. The adsorption minimum is at a DT site generated by the dangling bonds of the step-edge atoms (marked by the dark triangle). The difference between the two steps offers some clue on the dependence on the miscut angle θ experimentally observed if one assumes that the growth of θ changes the number of steps of a given type and this weakens the adsorption of the entire structure. This possibility is also considered in [5].

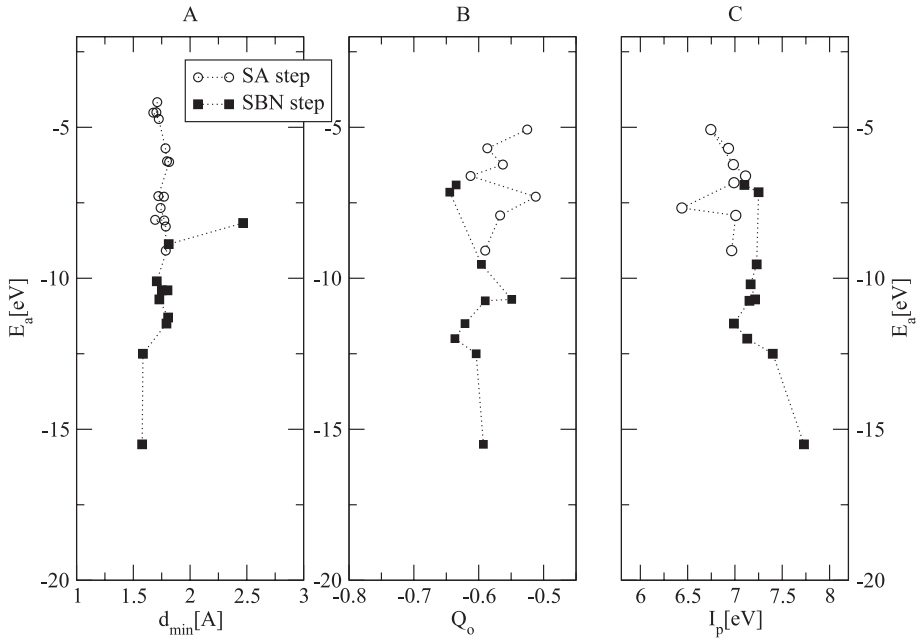

Fig. 4. The figure shows the functional dependence of E_a on d_{min}, Q_o and I_p.

The properties of the electronic structure of the oxygen-absorbed steps are summarized by Figure 4. The figure shows the functional dependence of E_a on d_{min} (which is the shortest Si-O distance) and on the Mulliken charge and ionization potential, Q_o and I_p, respectively. These calculations emphasize the difference between the two steps and add detail to the properties described above.

Though the values of d_{min}, Q_o and I_p are essentially similar in the two steps, the E_a values are different and a stronger adsorption is observed on SBN. On SA adsorption occurs prevalently on terraces via DB and BB sites. Therefore the values of E_a on SA reproduce the ones obtained for the flat surface (for Si(100)2×1 these values are in the range $-6, -8$ eV [10]) as the atomic arrangement is equal in the two cases. Furthermore d_{min} is similar for both DB and BB and its value agrees within a few per cent with the bond length of SiO (*i.e.* between 1.6 and 1.9 Å. Similar values are reported [2,10]). This accounts for the limited range of values of d_{min} on this step. On the contrary, on SBN adsorption occurs both on the terraces and at the step edge and all the four locations mentioned above are possible. The result is a broader range of d_{min} on SBN than on SA.

For steps, as for the flat surface, the adsorption capability has both an electrostatic and an elastic origin. The first one is dictated by the coulombic step-adsorbate interactions whereas the second one depends on the extent of the lattice relaxation. The slightly larger (absolute) values of Q_o on SBN are indicative of the greater strength of the electrostatic effects in this step. Also a more extensive relaxation can be deduced by the weaker bonding between the two terraces which reduces the step cohesive strength and increases its tendency to yield. Both effects account for the lower E_a on SBN. The plots in Figure 4 show also that on SBN the decrease of E_a is paralleled by the increase of I_p. The straightforward interpretation of this effect is the formation of deeply bounded step-edge states near the DT site. In agreement with this interpretation in [10] it is reported the presence of bands induced by the adsorbed oxygen.

To conclude this section it is added that the calculations using the smaller steps showed that: (i) serious problems of stability and unrealistically disordered steps are obtained only for the smaller steps with one dimer row and a few dimers in it, (ii) in all the other cases the E_a values reproduce the ones obtained for the larger steps without evident size-dependent effects.

5 Conclusion

In conclusion, this study has shown the effects of SA and SBN steps on oxygen adsorption. It is though that this study moves a step further from the traditional situation examined in adsorption which limits the structure of the exposed surface to a low-index surface of variable orientation. It is hoped that this elicits further studies based on more refined Hamiltonians and more experiments to add depth to the results reported here and to validate present and future calculations.

This work has been financially supported by the FIRB program under cotract RBAU01M9TL.

References

1. K. Kato, T. Uda, K. Terakura, Phys. Rev. Lett. **80**, 200 (1998)
2. Y. Widjaja, C.B. Musgrave, J. Chem. Phys. **116**, 5774 (2002)
3. C. Ebner, J.V. Seiple, J.P. Pelz, Phys. Rev. B **52**, 16651 (1995)

4. J.V. Seiple, C. Ebner, J.P. Pelz, Phys. Rev. B **53**, 15432 (1996)
5. V. Brichzin, J.P. Pelz, Phys. Rev. B **59**, 10138 (1999)
6. D.E. Jones, J.P. Pelz, Y. Hong, E. Bauer, I.S. Tsong, Phys. Rev. Lett. **77**, 330 (1996)
7. C. Ebner, D.E. Jones, J.P. Pelz, Phys. Rev. B **56**, 1581 (1997)
8. A.M. Mazzone, Comp. Mat. Science **223**, 213 (2001)
9. H. Watanabe, K. Kato, T. Uda, K. Fujita, M. Ichikawa, T. Kawamura, K. Terakura, Phys. Rev. Lett. **80**, 345 (1998)
10. Y. Miyamoto, A. Oshiyama, Phys. Rev. B **41**, 12680 (1990)
11. T. Uchiyama, M. Tsukada, Phys. Rev. **53**, 7917 (1996)
12. D.J. Chadi, Phys. Rev. Lett. **59**, 1691 (1987)
13. H.A. Duarte, D.R. Salahub, J. Chem. Phys. **108**, 743 (1998)
14. MOPAC Quantum Chemistry Program Exchange: Program Number 571. Method, options and tests on MOPAC are described by M.S.J. Dewar, W.J. Thiel, J. Am. Chem. Soc. **99**, 4899 (1977); J.P. Stewart, J. Comput. Chem. **10**, 209 (1989). Other information can be found at the web site `www.indiana.edu`
15. J. Shoemaker, L.W. Burggraf, M.S. Gordon, J. Chem. Phys. **112**, 2994 (2000)
16. M.R. Pederson, W.E. Pickett, S.C. Erwin, Phys. Rev. B **48**, 17400 (1993)
17. A.B. Filonov, A.N. Kholod, V.E. Borisenko, A.L. Pushkarchuk, V.M. Zelenkovskij, F. Bassani, F. Arnaud d'Avitaya, Phys. Rev. B **57**, 1394 (1998)
18. A.I. Boldyrev, J. Simmons, J. Phys. Chem. **97**, 5875 (1993)
19. A.I. Boldyrev, J. Simmons, V. Zakrzewski, W. Niessen, J. Phys. Chem. **98**, 1427 (1994)
20. L.S. Wang, J.N. Nichols, M. Dupuis, H. Wu, S.D. Colson, Phys. Rev. B **78**, 4450 (1997)
21. A. Oshiyama, Phys. Rev. Lett. **74**, 130 (1994)
22. P. Boguslawski, Q.M. Zhang, Z. Zhang, J. Bernholc, Phys. Rev. Lett. **72**, 3694 (1994)
23. E. Pehlke, P. Kratzer, Phys. Rev. B **59**, 2790 (1999)
24. D.R. Bowler, M.G. Bowler, Phys. Rev. B **57**, 15385 (1998)
25. E. Wimmer, H. Krakauer, M. Weinert, A.J. Freeman, Phys. Rev. B **2**, 864 (1981)
26. K. Raghavachari, V. Logovinsky, Phys. Rev. Lett. **55**, 2853 (1985)